FOLIA HISTOCHEMICA ET CYTOBIOLOGICA
Vol. 61, No. 3, 2023
pp. 172–182

ORIGINAL PAPER

VIA MEDICA

Inhibition of autophagy promotes sonodynamic therapy-induced apoptosis of pancreatic cancer cells

Xiaoxue Du, Jiaming Song, Ziwen Zhang, Jia Liu, Dan Xu

Department of Gastrointestinal Oncology, Harbin Medical University Cancer Hospital, Harbin, P.R. China

Abstract

Introduction. Sonodynamic therapy (SDT), a promising non-invasive therapeutic modality, has attracted increasing attention in the treatment of pancreatic cancer (PC). At present, the role of autophagy in SDT of PC remains unclear. This study aims to explore the role of autophagy in SDT of PC and its effect on apoptosis of PC cells.

Material and methods. PC cells (Capan-1 and BxPC-3) underwent incubation with 5-aminolevulinic acid (5-ALA) or/and ultrasound (US) exposure (control, 5-ALA, US, and SDT groups), followed by measurement of cell apoptosis and autophagy. Specifically, cell viability, apoptosis, and the expression of apoptosis-related proteins (cleaved Caspase-3, Bax, and Bcl-2) were measured using CCK-8 assay, flow cytometry, and western blot analysis, respectively. The mitochondrial morphology was observed with the transmission electron microscopy, accompanied by the detection of autophagosome marker (LC3) co-located with Mito and the protein expression of LC3II/I. Before SDT treatment, the autophagy inhibitor 3-MA and the apoptosis inhibitor z-VAD were respectively added to PC cell cultures to evaluate the effects of autophagy inhibition on apoptosis and apoptosis inhibition on autophagy in PC cells.

Results. Compared with the control group, cell viability was inhibited and cell apoptosis and autophagy were enhanced in the SDT group, while cell viability, autophagy, and apoptosis in the 5-ALA and US groups were not significantly changed. Moreover, 3-MA treatment inhibited autophagy and accelerated apoptosis, whereas z-VAD treatment reduced apoptosis but did not affect autophagy in PC cells.

Conclusions. Autophagy was activated in SDT-treated PC cells, and inhibition of autophagy promoted cell apoptosis in PC cells. *(Folia Histochemica et Cytobiologica 2023, Vol. 61, No. 3, 172–182)*

Keywords: Pancreatic cancer cell lines; sonodynamic therapy; autophagy; apoptosis; 5-aminolevulinic acid; inhibitors

Introduction

Pancreatic cancer (PC) is a highly lethal gastrointestinal cancer with a 5-year survival rate of < 5% [1], and its morbidity and mortality are increasing year by year worldwide [2]. Obesity, smoking, diabetes, alcohol, diet, and infection are widely-recognized risk factors associated with PC [3]. Notably, PC often fails to be diagnosed at an early stage, and most patients already suffer from tumor micro-metastases at the time of initial diagnosis [4]. At present, the conventional therapies of PC are mainly surgery, chemotherapy, radiotherapy, and combination therapy, but these therapies have shortcomings such as low selectivity, systemic toxicity, and drug resistance [5–7]. Therefore, mounting efforts are needed to develop new treatments for PC.

Sonodynamic therapy (SDT) is a non-invasive therapeutic modality for malignant tumors using a combination of sonosensitizers and low-intensity ultrasound (US) [8], which is developed from photodynamic therapy (PDT). Compared to PDT, SDT has many advantages, including deeper tissue penetration, high precision, less side effects, and favorable patient compliance [9]. In recent years, the role of SDT in

Correspondence address:
Xiaoxue Du
Department of Gastrointestinal Oncology
Harbin Medical University Cancer Hospital
150 Haping St, Nangang District, Harbin, Heilongjiang, 150081, P.R. China
Phone/fax: +8613654558264
e-mail: duxiaoxueo_o@163.com

Folia Histochem Cytobiol. 2023
10.5603/fhc.95262
ISSN 0239-8508, e-ISSN 1897-5631

www.journals.viamedica.pl/folia_histochemica_cytobiologica

tumor therapy has attracted increasing attention. Existing evidence has confirmed that SDT can effectively act on a variety of tumor cells, such as breast cancer [10], non-small-cell lung cancer [11], hepatocellular carcinoma [12], ovarian cancer [13], glioblastoma [14], prostate cancer [15], and PC [16]. Reportedly, the anti-tumor mechanism of SDT mainly involves reactive oxygen species (ROS) generation, apoptosis, and autophagy [9, 17].

Autophagy is a self-digestion process of the cell, in which damaged or senescent proteins and organelles in cells are wrapped in autophagosomes with a bilayer membrane structure and then transported to lysosomes for degradation [18]. Autophagy is involved in numerous functions including cell growth, survival, and death both in normal and cancer cells [19]. Mitochondria are important sites for energy metabolism and adenosine triphosphate production [20]. Autophagy can have both positive and negative effects, and selective autophagy is an evolutionarily conserved mechanism that removes excess protein aggregates and damaged intracellular components [21]. During SDT, autophagy may protect against or cause cell death [22]. SDT can decrease the survival rate of PC cells while inducing cell apoptosis, necrosis, and cytotoxicity [23]. However, little is known regarding the role of autophagy in SDT-induced PC cells. Herein, this study investigates the mechanism underlying the anti-cancer effects of SDT in two PC cell lines and the crosstalk of apoptosis and autophagy in SDT-induced PC cells.

Material and methods

Cell culture. Human PC cells, Capan-1 (Laboratory of Medical Genetics, Department of Biology, Harbin Medical University, China) and BxPC-3 [American Type Culture Collection (ATCC), Manassas, VA, USA], were incubated in Roswell Park Memorial Institute-1640 (RPMI) medium (ATCC) with 10% fetal bovine serum (FBS) at 37°C and in the atmosphere of 5% CO_2. The culture method was suspension culture, and the medium was refreshed 2~3 times a week.

Ultrasonic device. As described in our previous study [23], the US transducer, ultrasonic generator, and power amplifier used in our study were assembled by the Harbin Institute of Technology (Harbin, China). A petri dish with a lid containing target cells was placed above the US transducer and partially soaked in water (Fig. 1). For sonication, water was adopted as an ultrasonic coupling medium and also assisted in diminishing the thermal impact of ultrasonic irradiation. The temperature of the medium was monitored by a temperature measuring instrument in the US and SDT cell line groups, and no obvious temperature change was observed during the experiment (± 1°C).

Cell grouping and treatment. The concentration of 5-aminolevulinic acid (5-ALA; Sigma-Aldrich, St. Louis, MO, USA) and the intensity and exposure time to US were referred to our previous study [23] combined with another reference [24]. Capan-1 and BxPC-3 cells were allocated into six groups: control [6-h incubation with phosphate-buffered saline (PBS)], 5-ALA group [6-h incubation with 1 mmol/L 5-ALA (dissolved in PBS)], US group [6-h incubation with PBS and 5-min exposure to US (resonance frequency = 1.0 MHz, duty factor = 60%, intensity = 2 W/cm^2)], SDT group (6-h incubation with 1 mmol/L 5-ALA and 5-min exposure to US under the same conditions as the US group), SDT + 3-Methyladenine (3-MA) group [incubation with 1 mM 3-MA dissolved in DMSO (Merck Millipore, Billerica, MA, USA) for 1 h [22] and with 1 mmol/L 5-ALA for 6 h, followed by US treatment], and SDT+ z-VAD--fmk (z-VAD) group [incubation with 10 μM z-VAD dissolved in DMSO (Merck Millipore) for 1 h [22] and with 1 mmol/L 5-ALA for 6 h, followed by the US treatment].

Cell counting kit 8 (CCK-8). The cells were seeded onto a 96-well plate with 100 μL diluted cell suspensions (5×10^5 cells/mL) *per* well. Three replicate wells were set for each sample. Subsequent to 24 h of cell incubation, 10 μL CCK-8 reagents (Sigma-Aldrich) was added to each well for further 2 h. The absorbance was measured at 450 nm using SpectraMax iD5 multi-mode microplate reader (Molecular Devices, Downingtown, PA, USA) and analyzed using SoftMax Pro software.

Flow cytometry. Cell apoptosis was determined by an Annexin V-fluorescein isothiocyanate (FITC)/propidium iodide (PI) apoptosis detection kit (40302ES20, Yeasen, China). Briefly, cells were collected after trypsin digestion and centrifugation (1500 r/min, 5 min), followed by resuspension in PBS. Afterward, cell suspension (5×10^5 cells) was harvested and then centrifuged for 5 min at 1500 r/min, with the supernatant discarded. Next, the obtained cells were suspended in a binding buffer and then incubated with 5 μL of Annexin V-FITC for 15 min (4°C) and then 10 μL of PI for 5 min (at room temperature, in dark). Finally, a flow cytometer BD LSRFortessaTM flow cytometer (BD Biosciences, Franklin Lakes, NJ, USA) was utilized to measure cell apoptosis and BD AccuriTM C6 program was used for data analysis. The maximum excitation wavelength of FITC is 488 nm and the maximum emission wavelength is 525 nm. The PI-DNA complex has a maximum excitation wavelength of 535 nm and a maximum emission wavelength of 615 nm. Each sample included 10000 events.

Transmission electron microscopy (TEM). After twice washes with 1 × PBS, the cells were digested with 1 mL 0.25% trypsin for 2 min. After that, cell suspension of each group was collected into a 1.5 mL Eppendorf centrifuge tube, fixed in 4.2% glutaraldehyde for 2 h and then 30% osmium tetroxide solution for 1 h, followed by dehydration in gradient alcohol (100–24%) and epoxypropane. Later, the cells underwent embedding in Epon 812 and sectioning (80 nm) with an ultra-microtome (LKB Produkter, Bromma, Sweden). Following uranyl acetate and lead citrate staining, the ultrastructure of mitochondria was observed under the JEM-1400 electron microscope (Jeol, Tokyo, Japan). Damaged mitochondria are characterized by rupture of inner

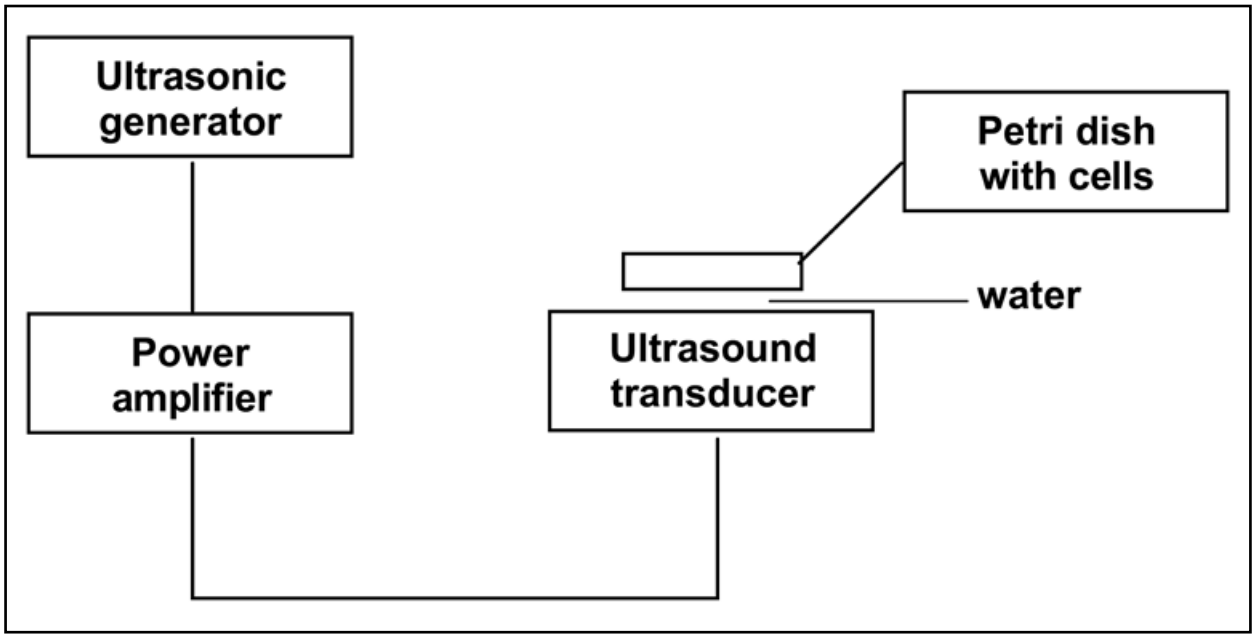

Figure 1. Schematic diagram of the ultrasonic device

and outer membranes, mitochondrial swelling, loss or rupture of cristae, and presence of autophagosomes.

Immunofluorescence of light chain 3 (LC3). The slide with the cells in the petri dish was soaked in PBS 3 times. After the slide was fixed in 4% formaldehyde, the cells underwent overnight (4°C) incubation with primary antibody anti-LC3 (ab192890, 1 μg/mL, Abcam, Cambridge, UK). After PBS washing, the sections were treated by the fluorescence-labeled secondary antibody IgG H&L (Alexa Fluor® 488) (ab150077, 1 μg/mL, Abcam) for 2 h in dark. After 4',6-diamidino-2-phenylindole (DAPI) staining, the sections were observed under TCSSP2 laser confocal fluorescence microscope (magnification: 400×) (Leica, TCSSP2, Germany) and analyzed using Leica LAS AF software. Excitation (Ex) and emission (Em) filters (from Semrock, Lake Forest, IL, USA) were as follows: DAPI (Ex/ /Em = 350/470 nm), LC3 (Ex/Em = 495/519 nm). LC3/DAPI fluorescence intensity ratio was used for quantitative analysis, and the fluorescence intensity was normalized to the LC3/DAPI intensity of the control group.

Western blot analysis. The cells were subjected to three washes with pre-cooled PBS and treatment with radio-immunoprecipitation assay cell lysis (Beyotime, Shanghai, China), followed by protein concentration estimation with a bicinchoninic acid protein assay kit (Beyotime). Proteins were mixed with the loading buffer (Beyotime), denatured in a boiling-water bath for 3 min, and separated by electrophoresis (80 V for 30 min and 120 V for 1–2 h). Next, the proteins were electro-blotted for 60 min to membranes in an ice bath at 300 mA. Afterward, the membranes were rinsed in washing solution for 1–2 min and sealed in blocking solution at room temperature for 60 min or at 4°C overnight. Next, the membranes received 1-h probing with primary antibodies from Abcam against cleaved Caspase-3 (ab32042, 1:500), B-cell lymphoma-2 (Bcl-2; ab182858, 1:2000), Bcl-2 associated X (Bax; ab32503, 1:1000), LC3 (ab128025, 1:1000), and GAPDH (ab9485, 1:2500). After washing (3 × 10 min), the membranes were subjected to 1-h re-probing with immunoglobulin G (IgG; 1:1000, Abcam) antibodies and washed three times (3 × 10 min). Lastly, a chemiluminescent imaging system (Bio-rad, Hercules, CA, USA) was used for detection after color development. The assays were performed thrice.

Statistical analysis. Statistical analysis of the collected original data was conducted with GraphPad Prism (version 8.0) software (GraphPad Inc, San Diego, CA, USA) and presented as mean ± standard deviation. For the samples conforming to normal distribution, the Student's *t*-test was employed for two-group comparisons, and the one-way analysis of variance for comparisons among multiple groups. The Tukey's test was used for *post hoc* multiple comparison. A P value < 0.05 was considered statistically significant.

Results

SDT induced cell apoptosis in PC cells

In our previous study, incubation with 5-ALA (1 mmol/L, 6 h) combined with US exposure (2 W/ /cm^2, 5 min) could induce cytotoxicity and apoptosis of PC Capcan-1 cells [23]. However, the time change of cytotoxicity and apoptosis after SDT treatment has not been clarified in Capan-1 and BxPC-3 cell lines. Therefore, CCK-8 assay was performed at different time points (0, 2, 4, and 12 h) after treatment with

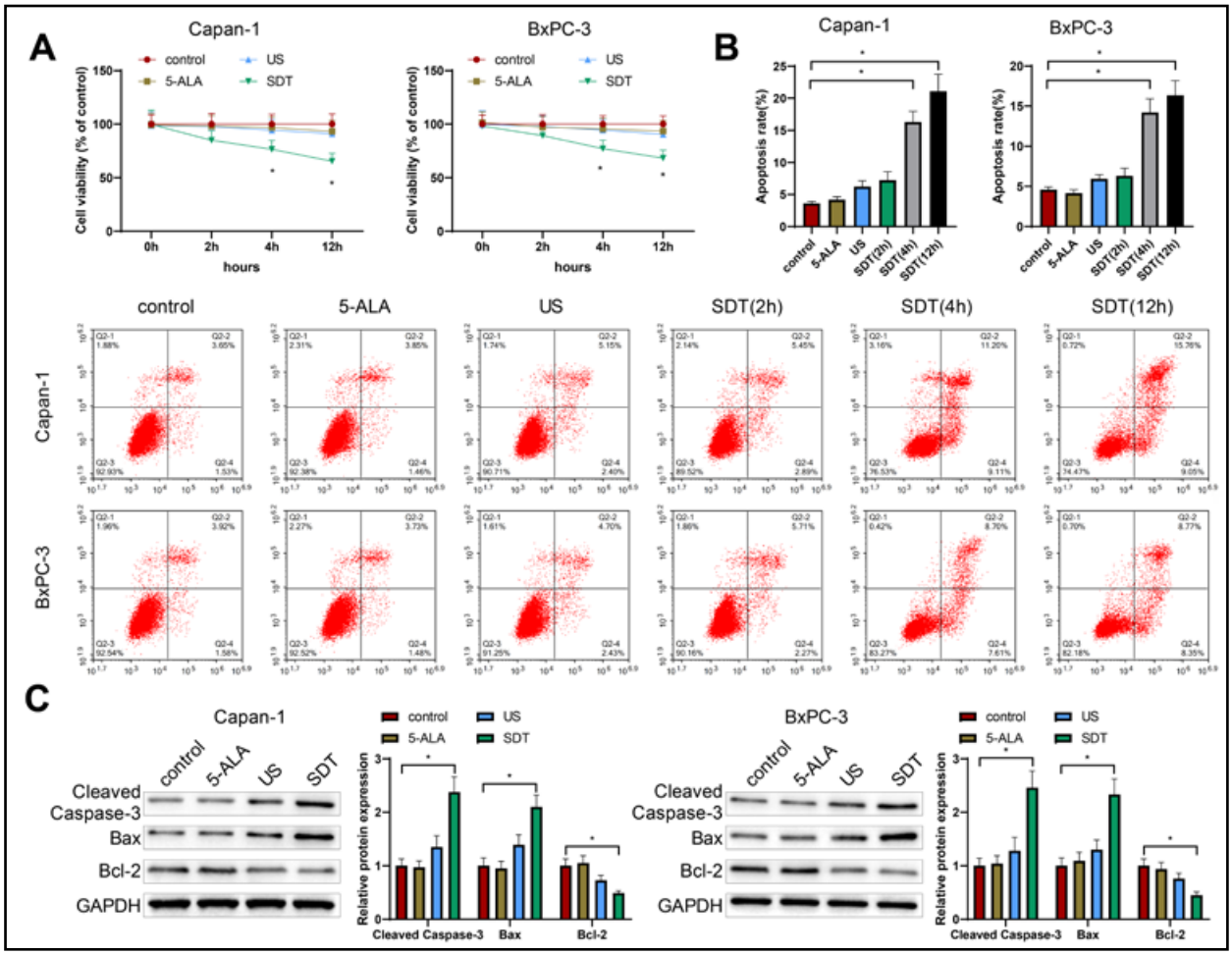

Figure 2. SDT increased the apoptotic rate of Capan-1 and BxPC-3 pancreatic cancer (PC) cells. **A.** CCK-8 assay was used to measure cell viability of PC cells at different time points (0, 2, 4, and 12 h) after treatment in each group. **B.** Flow cytometry was used to test cell apoptosis of PC cells in the SDT group at 2, 4, 12 h, and the other three groups at 4 h after treatment. **C.** The expression of apoptosis-related proteins (cleaved Caspase-3, Bax, and Bcl-2) in each group was assessed through western blot analysis. $^{*}P < 0.05$, compared with the control group. Abbreviations: 5-ALA — 5-aminolevulinic acid; Bax — Bcl-2 associated X; Bcl-2 — B-cell lymphoma-2; CCK-8 — cell counting kit 8; SDT — sonodynamic therapy; US — ultrasound.

5-ALA, and the results showed that compared with the control group (cell viability: 100%), cell viability did not markedly change in the 5-ALA and US groups at different time points but substantially declined in the SDT group at 4 h (Capan-1 cells: 76.45%; BxPC-3 cells: 77.09%) and 12 h (Capan-1: 65.39%; BxPC-3: 68.33%) after treatment (Fig. 2A). Next, flow cytometry was carried out to detect cell apoptosis in the cells of SDT group incubated for 2, 4, and 12 h with 5-ALA and the other three groups at 4 h after treatment. As manifested in Fig. 2B (*vs*. the control group), cell apoptosis was not markedly altered in the 5-ALA group, insignificantly augmented in the US group, and substantially elevated in the SDT group at 4 h and 12 h. These results suggested that the apoptotic rate of PC cells increased markedly after 4 h of SDT treatment and increased with time, but the increase was slow after 4 h. Therefore, PC cells at 4 h after treatment were used for subsequent experiments. Furthermore, data from western blot analysis manifested that versus the control group, cleaved Caspase-3 and Bax expression strikingly increased but Bcl-2 expression decreased in the SDT group, while the levels of these proteins did not significantly change in the 5-ALA and US groups (Fig. 2C). These results indicated that SDT treatment induced PC cell apoptosis.

SDT induced autophagy of PC cells

Next, the effect of SDT on autophagy in PC cells was probed. TEM results revealed that there was no obvious change in the autophagy level of cells in the control and 5-ALA groups, a small number of autophagosomes appeared in the US group, and the number of autophagosomes in the SDT group increased significantly (Fig. 3A). Immunofluorescence staining results showed that the expression of autophagosome marker

(LC3) was conspicuously increased in the cells of the SDT group but did not substantially change in the 5-ALA and US groups (*vs*. the control group, Fig. 3B). As for the results of western blot analysis, the protein expression of LC3II/I was elevated in the SDT group but did not significantly change in the 5-ALA and US groups (*vs*. the control group, Fig. 3C). Taken together, SDT treatment triggered autophagy in PC cells.

Inhibition of SDT-induced autophagy promoted PC cell apoptosis

Subsequently, we dissected the effect of autophagy inhibition on PC cell apoptosis. First, the CCK-8 assay revealed that cell viability in the SDT group was clearly repressed compared with that in the control group. Moreover, cell viability was substantially reduced in the SDT + 3-MA group versus the SDT group (Fig. 4A). Meanwhile, the SDT group exhibited an elevation in cell apoptosis as compared to the control group. In addition, further increase in cell apoptosis was observed in the SDT + 3-MA group (*vs*. the SDT group) and decreased cell apoptosis was found in the SDT + z-VAD group (*vs*. the SDT group) (Fig. 4B). As reflected by western blot analysis, the SDT group had increased expression of cleaved Caspase-3 and Bax but decreased expression of Bcl-2 (*vs*. the control group), and the same trend was observed in the SDT + 3-MA group versus the SDT group. However, cleaved Caspase-3 expression substantially declined, and Bcl-2 and Bax expression did not significantly change in the SDT + z-VAD group (*vs*. the SDT group) (Fig. 4C). These findings demonstrated that the autophagy inhibitor 3-MA could accelerate PC cell apoptosis induced by SDT.

Inhibition of SDT-induced cell apoptosis did not affect autophagy in PC cells

Finally, we further investigated the effect of apoptosis inhibition on autophagy of PC cells. From TEM observation, the autophagy level in the SDT group was significantly increased compared with the control group. In comparison with the SDT group, the autophagy level in the SDT + z-VAD group did not change significantly but markedly decreased in the SDT + 3-MA group (Fig. 5A). Immunofluorescence staining indicated that LC3 expression was markedly elevated in the SDT and SDT + z-VAD groups (*vs*. the control group), but there was no significant difference between these two groups; compared with the SDT group, the SDT + 3-MA group had reduced expression of LC3 (Fig. 5B). Western blot analysis exhibited that the SDT and SDT + z-VAD groups had increased LC3II/I content (*vs*. the control group), while the SDT + 3-MA group had reduced LC3II/I expression as compared to the SDT group. No marked difference was found in LC3II/I expression between the SDT and SDT + z-VAD groups (Fig. 5C). In summary, the autophagy inhibitor could inhibit SDT-induced autophagy in PC cells, but the apoptosis inhibitor did not affect SDT-induced autophagy.

Discussion

PC is a severe disease that threatens human health, with limited treatment options [25]. Nowadays, SDT has a wide board development space for treatment of PC [26]. Theoretically, SDT combines US with sonosensitizers, in which US is used to penetrate deep tissues to focus on specific areas, thus activating the sonosensitizers that are enriched in the tumor tissues and finally promoting the production of ROS to induce cell apoptosis [27]. Moreover, SDT has been verified to trigger autophagy and apoptosis [28]. In the present study, we evaluated the effect of SDT intervention on PC cell apoptosis and autophagy and found that SDT induced PC cell apoptosis and autophagy. Further experiments illustrated that autophagy inhibition facilitated SDT-induced apoptosis, but apoptosis cannot affect SDT-induced autophagy in PC cells (Fig. 6).

5-ALA is often utilized as porphyrin-based sonosensitizers in *in vivo* and *in vitro* models for SDT [29, 30]. We previously found that incubation with 5-ALA followed by US exposure could trigger cell cytotoxicity and apoptosis [23]. In this study, we used 5-ALA or/and US to treat PC cells and found that SDT treatment significantly increase the apoptotic rate of PC cells, accompanied by enhanced expression of cleaved Caspase-3 and Bax, pro-apoptotic factors, and reduced expression of Bcl-2, a major anti-apoptotic factor [31, 32]. Consistently, Yang *et al.* demonstrated that ALA loaded lipid/poly (lactic-co-glycolic acid) microbubble-mediated SDT increased the apoptotic rate and enhanced ROS levels in PC cells, suggesting the anti-tumor effect of 5-ALA-mediated SDT on PC cells [33]. Mitochondrial and nuclear DNA mutations caused by oxidative damage can result in mitochondrial ROS production, forming a 'vicious cycle' between mitochondria, ROS, and cancer development [34]. The mitochondrial pathway of apoptosis is activated following cellular stress [35]. Increasing evidence revealed that ROS generated within mitochondria can drive oxidative damage, inflammatory signaling, and cell apoptosis [36, 37]. Specifically, damaged mitochondria may induce overproduction of ROS, trigger the release of cytochrome C, or activate the levels of some pro-apoptotic factors, and finally induce cell apoptosis [35, 38]. Also, Suehiro S *et al.* illustrated that 5-ALA-SDT inhibited cell growth and

Folia Histochem Cytobiol. 2023
10.5603/fhc.95262
ISSN 0239-8508, e-ISSN 1897-5631

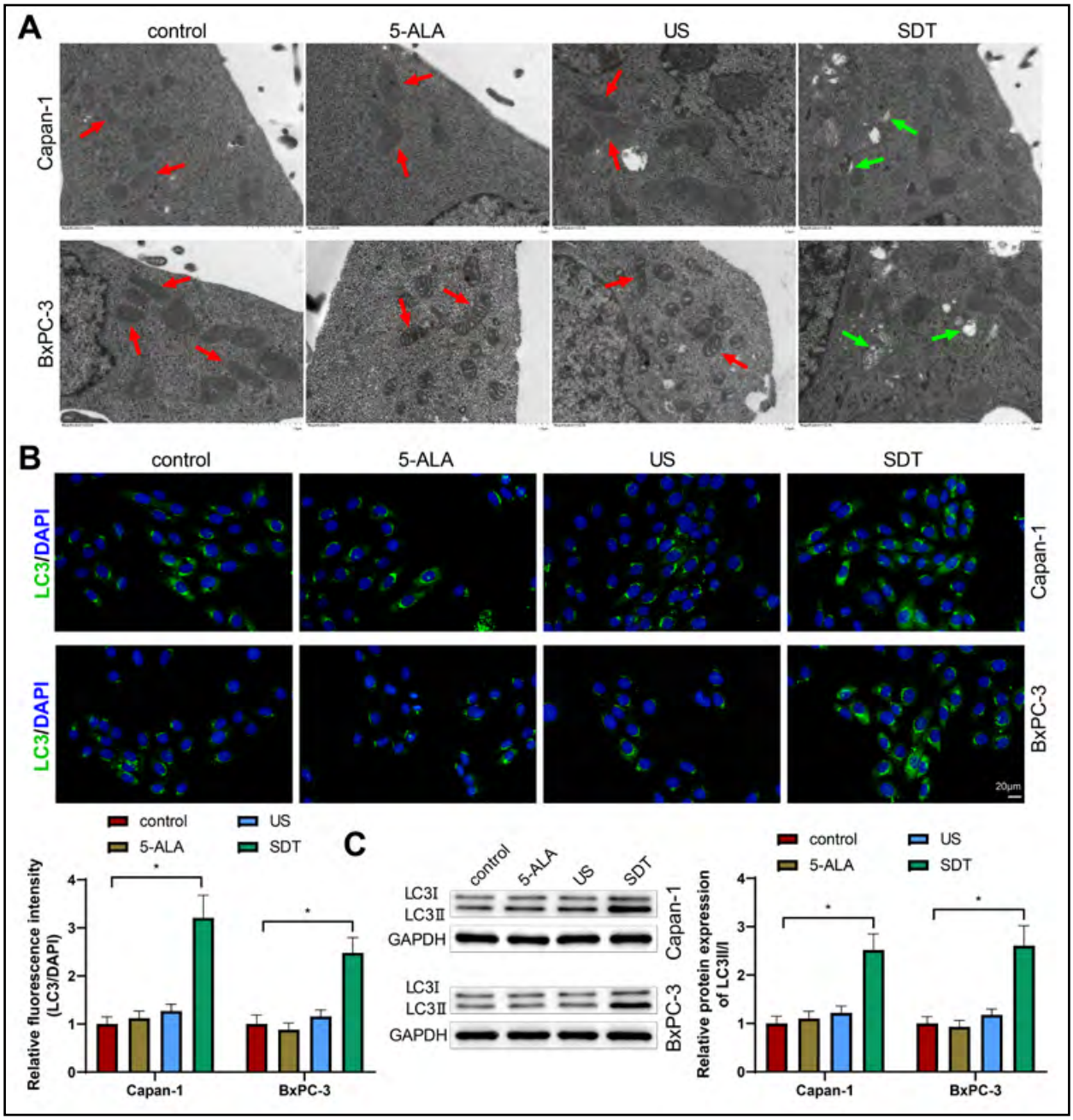

Figure 3. SDT increased autophagy in pancreatic cancer (PC) cells. **A.** Transmission electron microscopy was used to study the ultrastructure of PC cell treated by 5-ALA, US and SDT. Mitochondria are marked by red arrows and the autophagosomes by green arrows. **B.** Immunofluorescence staining was used to measure the expression of autophagosome marker LC3 protein. **C.** The protein expression of LC3II/I was measured by western blot analysis. $^{*}P < 0.05$, compared with the control group. Abbreviations: 5-ALA — 5-aminolevulinic acid; LC3 — light chain 3; SDT — sonodynamic therapy; US — ultrasound.

induced cell apoptosis and death in glioma cell models, serving as a less invasive and tumor-specific therapy in malignant gliomas [39].

In addition to apoptosis, we also investigated the effect of SDT on autophagy of PC cells. As expected, SDT treatment contributed to autophagy of PC cells, shown by the appearance of autophagosomes and the significant increase of LC3II/I expression. LC3II is a well-known marker of autophagy [40]. In a previous study of glioma therapy, SDT treatment induced apoptosis and MAPK/p38-PINK1-PRKN-dependent autophagy, and moreover, angiopep-2-modified liposomes loaded with Ce6 and hydroxychloroquine-SDT treatment could inhibit the xenograft-tumor growth and prolong the survival time of tumor-bearing mice [41]. Feng *et al.* observed that SDT triggered autophagy at low dosage, serving as a survival pathway for breast cancer and exhibiting resistance to SDT-media-

Folia Histochem Cytobiol. 2023
10.5603/fhc.95262
ISSN 0239-8508, e-ISSN 1897-5631

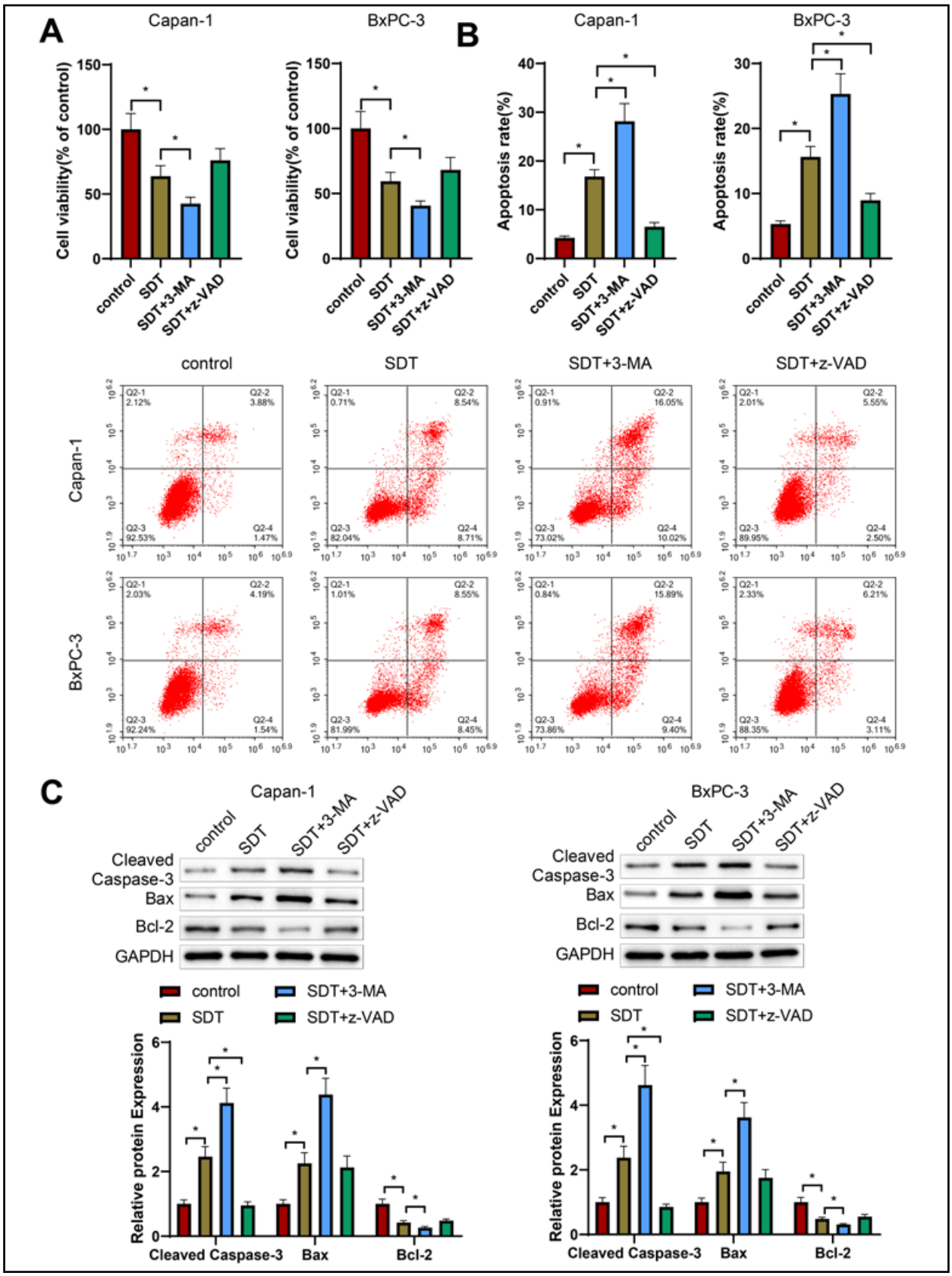

Figure 4. Repression of SDT-induced autophagy accelerated apoptosis in pancreatic cancer (PC) cells. **A.** Cell viability was evaluated using CCK-8 assay. **B.** Cell apoptosis was measured *via* flow cytometry. **C.** The expression of apoptosis-related proteins (cleaved Caspase-3, Bax, and Bcl-2) in each group was detected using western blot analysis. *P < 0.05, compared with the control or SDT group. Abbreviations: 3-MA — 3-Methyladenine; 5-ALA — 5-aminolevulinic acid; Bcl-2 — B-cell lymphoma-2; Bax — Bcl-2 associated X; CCK-8 — cell counting kit 8; SDT — sonodynamic therapy; US — ultrasound; z-VAD — z-VAD-fmk.

Folia Histochem Cytobiol. 2023
10.5603/fhc.95262
ISSN 0239-8508, e-ISSN 1897-5631

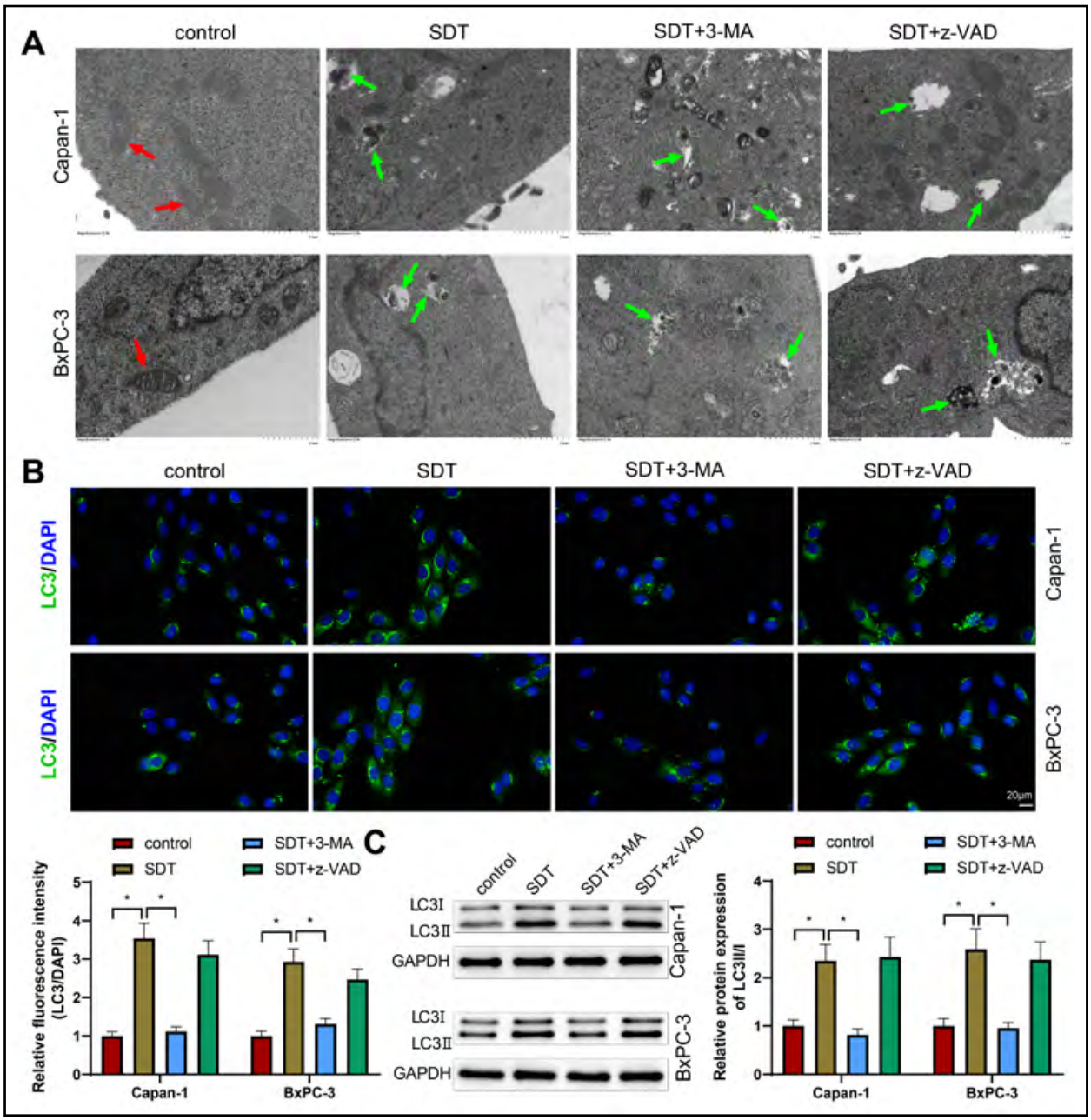

Figure 5. Suppression of SDT-induced cell apoptosis had no effect on autophagy in pancreatic cancer (PC) cells. **A.** Transmission electron microscopy was used to detect autophagosomes with the mitochondria marked by red arrows and the autophagosomes by green arrows. **B.** Immunofluorescence staining was used to demonstrate the expression of the autophagosome marker LC3. **C.** The relative content of LC3II/I was tested by western blot analysis. $^{*}P < 0.05$, compared with the control group. Abbreviations: 3-MA — 3-Methyladenine; 5-ALA — 5-aminolevulinic acid; LC3 — light chain 3; SDT — sonodynamic therapy; US — ultrasound; z-VAD — z-VAD-fmk.

ted apoptosis [42]. Consequently, it can be concluded that SDT treatment induces apoptosis and autophagy of PC cells simultaneously. Moreover, an earlier study indicated that autophagy blockade enhanced the anti-tumor effect of SDT *via* apoptosis and necrosis induction, while caspase inhibition did not affect the formation of autophagosomes or protect against SDT-triggered cytotoxicity, providing important insight into the combination of autophagy inhibitors and SDT for cancer treatment [43].

In cancer treatment, autophagy is like a double-edged sword, which can induce apoptosis to repress tumor progression and inhibit apoptosis to promote tumor cell growth [44, 45]. Chen *et al.* found that ketoconazole downregulated cyclooxygenase-2 expression and activated autophagy to induce apoptosis in hepatocellular carcinoma (HCC) cells [46]. Wang

Folia Histochem Cytobiol. 2023
10.5603/fhc.95262
ISSN 0239-8508, e-ISSN 1897-5631

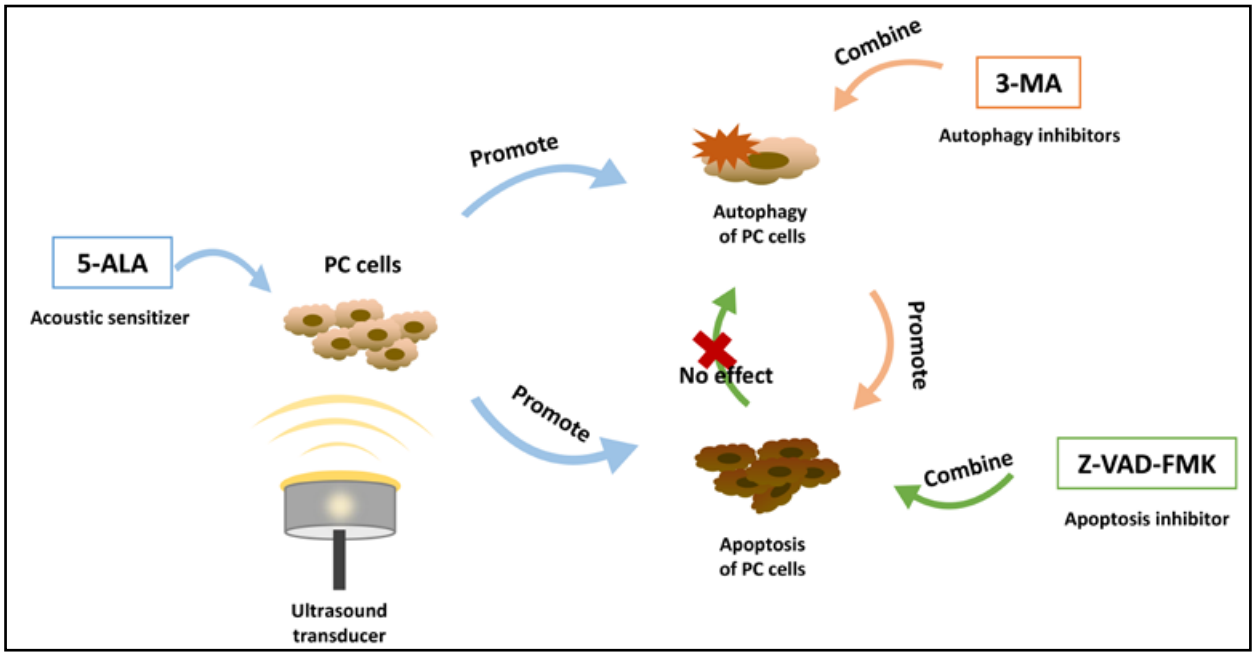

Figure 6. A graphical summary of the results shows that inhibition of autophagy promotes sonodynamic therapy-induced apoptosis of pancreatic cancer (PC) cells. 5-ALA incubation and ultrasound exposure induced autophagy and apoptosis of PC cells. 3-MA treatment inhibited autophagy and accelerated apoptosis, whereas z-VAD treatment reduced apoptosis but did not affect autophagy in PC cells. Abbreviations: 3-MA — 3-Methyladenine; 5-ALA — 5-aminolevulinic acid; PC — pancreatic cancer; z-VAD — z-VAD-fmk.

et al. observed that blocking autophagy significantly reduced mitochondrial potential and increased caspase-3 activity and cell apoptosis, finally enhanced the ability of SDT to induce cell death [47]. More importantly, a previous study revealed that suppression of autophagy could aggravate apoptosis and cell death induced by 5-ALA-SDT in human breast adenocarcinoma cells [24]. In our study, we used autophagy inhibitor 3-MA and apoptosis inhibitor z-VAD to probe the role of autophagy and apoptosis in SDT-treated PC cells. As expected, 3-MA treatment obviously promoted but z-VAD treatment repressed cell apoptosis induced by SDT. Similarly, in human leukemia K562 cells, SDT treatment induced ROS accumulation, cell apoptosis, and autophagy, while the presence of 3-MA or Ba A1 enhanced SDT-induced cell apoptosis [22]. However, our data unraveled that SDT-induced autophagy could be inhibited by the treatment with 3-MA but not be affected by z-VAD treatment. These data demonstrated that inhibition of SDT-induced autophagy promoted cell apoptosis, but inhibition of SDT-induced apoptosis did not affect autophagy in PC cells.

In this study, the obtained data demonstrated that treatment of 5-ALA-mediated SDT triggered PC cell apoptosis and autophagy, and inhibition of SDT-induced autophagy promoted PC cell apoptosis, suggesting that inhibition of autophagy may function as a potential therapeutic strategy to improve the efficiency of SDT. These findings may apply to SDT mediated by other sonosensitizers. Furthermore, since our research has only carried out at the cell level, the feasibility of the existing parametric mechanism of US in cell models needs to be further studied in animal models. Therefore, more animal and clinical trials are needed in the future, thereby providing experimental basis for the design of the novel therapies for PC.

Article information

Data availability statement

The datasets used or analyzed during the current study are available from the corresponding author on reasonable request.

Author contributions

DXX and SJM conceived the ideas. DXX, SJM, ZZW, LJ and XD designed the experiments. DXX, ZZW, LJ and XD performed the experiments. DXX, SJM, ZZW and XD analyzed the data. DXX, LJ and XD provided critical materials. DXX, SJM, ZZW, LJ and XD wrote the manuscript. DXX supervised the study. All the authors have read and approved the final version for publication.

10.5603/fhc.95262
ISSN 0239-8508, e-ISSN 1897-5631

Funding
This work was supported by the Scientific Research Project of Heilongjiang Provincial Health and Family Planning Commission (No. 2018248).

Conflict of interest
The authors declare there is no conflict of interests.

References

1. Li S, Xu HX, Wu CT, et al. Angiogenesis in pancreatic cancer: current research status and clinical implications. Angiogenesis. 2019; 22(1): 15–36, doi: 10.1007/s10456-018-9645-2, indexed in Pubmed: 30168025.
2. Hu JX, Zhao CF, Chen WB, et al. Pancreatic cancer: A review of epidemiology, trend, and risk factors. World J Gastroenterol. 2021; 27(27): 4298–4321, doi: 10.3748/wjg.v27.i27.4298, indexed in Pubmed: 34366606.
3. McGuigan A, Kelly P, Turkington RC, et al. Pancreatic cancer: A review of clinical diagnosis, epidemiology, treatment and outcomes. World J Gastroenterol. 2018; 24(43): 4846–4861, doi: 10.3748/wjg.v24.i43.4846, indexed in Pubmed: 30487695.
4. Jiang S, Fagman JB, Ma Y, et al. A comprehensive review of pancreatic cancer and its therapeutic challenges. Aging (Albany NY). 2022; 14(18): 7635–7649, doi: 10.18632/aging.204310, indexed in Pubmed: 36173644.
5. Yoshitomi H, Takano S, Furukawa K, et al. Conversion surgery for initially unresectable pancreatic cancer: current status and unresolved issues. Surg Today. 2019; 49(11): 894–906, doi: 10.1007/s00595-019-01804-x, indexed in Pubmed: 30949842.
6. Matsui H, Hazama S, Shindo Y, et al. Combination treatment of advanced pancreatic cancer using novel vaccine and traditional therapies. Expert Rev Anticancer Ther. 2018; 18(12): 1205–1217, doi: 10.1080/14737140.2018.1531707, indexed in Pubmed: 30295097.
7. Salazar J, Pérez-Bracchiglione J, Salas-Gama K, et al. Systemic Treatments for Advanced Digestive Cancer Research. Efficacy of systemic oncological treatments in patients with advanced pancreatic cancer at high risk of dying in the short or medium-term: overview of systematic reviews. Eur J Cancer. 2021; 154: 82–91, doi: 10.1016/j.ejca.2021.05.034, indexed in Pubmed: 34252759.
8. Son S, Kim JiH, Wang X, et al. Multifunctional sonosensitizers in sonodynamic cancer therapy. Chem Soc Rev. 2020; 49(11): 3244–3261, doi: 10.1039/c9cs00648f, indexed in Pubmed: 32337527.
9. Pan X, Wang H, Wang S, et al. Sonodynamic therapy (SDT): a novel strategy for cancer nanotheranostics. Sci China Life Sci. 2018; 61(4): 415–426, doi: 10.1007/s11427-017-9262-x, indexed in Pubmed: 29666990.
10. Huang C, Xu Y, Wang D, et al. Interference with redox homeostasis through a G6PD-targeting self-assembled hydrogel for the enhancement of sonodynamic therapy in breast cancer. Frontiers in Chemistry. 2022; 10, doi: 10.3389/fchem.2022.908892.
11. Qiu G, Xue L, Zhu X, et al. Cetuximab combined with sonodynamic therapy achieves dual-modal image monitoring for the treatment of egfr-sensitive non-small-cell lung cancer. Front Oncol. 2022; 12: 756489, doi: 10.3389/fonc.2022.756489, indexed in Pubmed: 35242698.
12. Yin H, Sun L, Pu Y, et al. Ultrasound-ControlledCRISPR/CAS9 system augments sonodynamic therapy of hepatocellular carcinoma. ACS Central Science. 2021; 7(12): 2049–2062, doi: 10.1021/acscentsci.1c01143.
13. Xie W, Zhu S, Yang B, et al. The destruction of laser-induced phase-transition nanoparticles triggered by low-intensity ultrasound: an innovative modality to enhance the immunological treatment of ovarian cancer cells. Int J Nanomedicine. 2019; 14: 9377–9393, doi: 10.2147/IJN.S208404, indexed in Pubmed: 31819438.
14. Wu T, Liu Y, Cao Yu, et al. Engineering macrophage exosome disguised biodegradable nanoplatform for enhanced sonodynamic therapy of glioblastoma. Adv Mater. 2022; 34(15): e2110364, doi: 10.1002/adma.202110364, indexed in Pubmed: 35133042.
15. Hadi MM, Nesbitt H, Masood H, et al. Investigating the performance of a novel pH and cathepsin B sensitive, stimulus-responsive nanoparticle for optimised sonodynamic therapy in prostate cancer. J Control Release. 2021; 329: 76–86, doi: 10.1016/j.jconrel.2020.11.040, indexed in Pubmed: 33245955.
16. Nesbitt H, Logan K, Thomas K, et al. Sonodynamic therapy complements PD-L1 immune checkpoint inhibition in a murine model of pancreatic cancer. Cancer Lett. 2021; 517: 88–95, doi: 10.1016/j.canlet.2021.06.003, indexed in Pubmed: 34119606.
17. McHale AP, Callan JF, Nomikou N, et al. Sonodynamic therapy: concept, mechanism and application to cancer treatment. Adv Exp Med Biol. 2016; 880: 429–450, doi: 10.1007/978-3-319-22536-4_22, indexed in Pubmed: 26486350.
18. Cao W, Li J, Yang K, et al. An overview of autophagy: mechanism, regulation and research progress. Bull Cancer. 2021; 108(3): 304–322, doi: 10.1016/j.bulcan.2020.11.004, indexed in Pubmed: 33423775.
19. Chen Y, Gibson SB. Three dimensions of autophagy in regulating tumor growth: cell survival/death, cell proliferation, and tumor dormancy. Biochim Biophys Acta Mol Basis Dis. 2021; 1867(12): 166265, doi: 10.1016/j.bbadis.2021.166265, indexed in Pubmed: 34487813.
20. Rencelj A, Gvozdenovic N, Cemazar M. MitomiRs: their roles in mitochondria and importance in cancer cell metabolism. Radiol Oncol. 2021; 55(4): 379–392, doi: 10.2478/raon-2021-0042, indexed in Pubmed: 34821131.
21. Zhang L, Dai L, Li D. Mitophagy in neurological disorders. J Neuroinflammation. 2021; 18(1): 297, doi: 10.1186/s12974-021-02334-5, indexed in Pubmed: 34937577.
22. Su X, Wang P, Yang S, et al. Sonodynamic therapy induces the interplay between apoptosis and autophagy in K562 cells through ROS. Int J Biochem Cell Biol. 2015; 60: 82–92, doi: 10.1016/j.biocel.2014.12.023, indexed in Pubmed: 25578562.
23. Li YJ, Huang P, Jiang CL, et al. Sonodynamically induced anti-tumor effect of 5-aminolevulinic acid on pancreatic cancer cells. Ultrasound Med Biol. 2014; 40(11): 2671–2679, doi: 10.1016/j.ultrasmedbio.2014.07.003, indexed in Pubmed: 25220273.
24. Song L, Huang Y, Hou X, et al. PINK1/Parkin-mediated mitophagy promotes resistance to sonodynamic therapy. Cell Physiol Biochem. 2018; 49(5): 1825–1839, doi: 10.1159/000493629, indexed in Pubmed: 30231241.
25. Hosein AN, Brekken RA, Maitra A. Pancreatic cancer stroma: an update on therapeutic targeting strategies. Nat Rev Gastroenterol Hepatol. 2020; 17(8): 487–505, doi: 10.1038/s41575-020-0300-1, indexed in Pubmed: 32393771.
26. Nicholas D, Nesbitt H, Farrell S, et al. Exploiting a rose bengal-bearing, oxygen-producing nanoparticle for SDT and associated immune-mediated therapeutic effects in the treatment of pancreatic cancer. Eur J Pharm Biopharm. 2021; 163: 49–59, doi: 10.1016/j.ejpb.2021.03.005, indexed in Pubmed: 33798727.
27. Nguyen Cao TG, Kang JiH, You JY, et al. Safe and targeted sonodynamic cancer therapy using biocompatible exosome-based nanosonosensitizers. ACS Appl Mater Interfaces. 2021; 13(22): 25575–25588, doi: 10.1021/acsami.0c22883, indexed in Pubmed: 34033477.
28. Zhang Y, Zhao Y, Zhang Y, et al. The crosstalk between sonodynamic therapy and autophagy in cancer. Frontiers in Pharmacology. 2022; 13, doi: 10.3389/fphar.2022.961725.

29. Peng Y, Jia L, Wang S, et al. Sonodynamic therapy improves antitumor immune effect by increasing the infiltration of CD8+ T cells and altering tumor blood vessels in murine B16F10 melanoma xenograft. Oncol Rep. 2018; 40(4): 2163–2170, doi: 10.3892/or.2018.6612, indexed in Pubmed: 30106435.
30. Shimamura Y, Tamatani D, Kuniyasu S, et al. 5-aminolevulinic acid enhances ultrasound-mediated antitumor activity via mitochondrial oxidative damage in breast cancer. Anticancer Res. 2016; 36(7): 3607–3612, indexed in Pubmed: 27354630.
31. Wang XX, Zhang B, Xia R, et al. Inflammation, apoptosis and autophagy as critical players in vascular dementia. Eur Rev Med Pharmacol Sci. 2020; 24(18): 9601–9614, doi: 10.26355/eurrev_202009_23048, indexed in Pubmed: 33015803.
32. Huang R, Xu Y, Lu Xi, et al. Melatonin protects inner retinal neurons of newborn mice after hypoxia-ischemia. J Pineal Res. 2021; 71(1): e12716, doi: 10.1111/jpi.12716, indexed in Pubmed: 33426650.
33. Yang W, Xu H, Liu Q, et al. 5-Aminolevulinic acid hydrochloride loaded microbubbles-mediated sonodynamic therapy in pancreatic cancer cells. Artif Cells Nanomed Biotechnol. 2020; 48(1): 1178–1188, doi: 10.1080/21691401.2020.1813743, indexed in Pubmed: 32924612.
34. Zhang Y, Yang B, Tu C, et al. Induction of mitochondria-mediated apoptosis in human gastric adenocarcinoma SGC-7901 cells by kuraridin and Nor-kurarinone isolated from Sophora flavescens. Asian Pac J Cancer Prev. 2011; 12(10): 2499–2504, indexed in Pubmed: 22320946.
35. Chen M, Yang J, Li L, et al. Metabolomics reveals that cysteine metabolism plays a role in celastrol-induced mitochondrial apoptosis in HL-60 and NB-4 cells. Sci Rep. 2020; 10(1): 471, doi: 10.1038/s41598-019-57312-y, indexed in Pubmed: 31949255.
36. Bugger H, Pfeil K. Mitochondrial ROS in myocardial ischemia reperfusion and remodeling. Biochim Biophys Acta Mol Basis Dis. 2020; 1866(7): 165768, doi: 10.1016/j.bbadis.2020.165768, indexed in Pubmed: 32173461.
37. Luo Z, Xu X, Sho T, et al. ROS-induced autophagy regulates porcine trophectoderm cell apoptosis, proliferation, and differentiation. Am J Physiol Cell Physiol. 2019; 316(2): C198–C209, doi: 10.1152/ajpcell.00256.2018, indexed in Pubmed: 30485137.
38. Ma K, Chen G, Li W, et al. Mitophagy, mitochondrial homeostasis, and cell fate. Front Cell Dev Biol. 2020; 8: 467, doi: 10.3389/fcell.2020.00467, indexed in Pubmed: 32671064.
39. Suehiro S, Ohnishi T, Yamashita D, et al. Enhancement of antitumor activity by using 5-ALA-mediated sonodynamic therapy to induce apoptosis in malignant gliomas: significance of high-intensity focused ultrasound on 5-ALA-SDT in a mouse glioma model. J Neurosurg. 2018; 129(6): 1416–1428, doi: 10.3171/2017.6.JNS162398, indexed in Pubmed: 29350596.
40. Yang H, Shen H, Li J, et al. SIGMAR1/Sigma-1 receptor ablation impairs autophagosome clearance. Autophagy. 2019; 15(9): 1539–1557, doi: 10.1080/15548627.2019.1586248, indexed in Pubmed: 30871407.
41. Qu F, Wang P, Zhang K, et al. Manipulation of Mitophagy by "All-in-One" nanosensitizer augments sonodynamic glioma therapy. Autophagy. 2020; 16(8): 1413–1435, doi: 10.1080/15548627.2019.1687210, indexed in Pubmed: 31674265.
42. Feng Q, Yang X, Hao Y, et al. Cancer cell membrane-biomimetic nanoplatform for enhanced sonodynamic therapy on breast cancer via autophagy regulation strategy. ACS Appl Mater Interfaces. 2019; 11(36): 32729–32738, doi: 10.1021/acsami.9b10948, indexed in Pubmed: 31415145.
43. Wang X, Wang P, Zhang K, et al. Initiation of autophagy and apoptosis by sonodynamic therapy in murine leukemia L1210 cells. Toxicol In Vitro. 2013; 27(4): 1247–1259, doi: 10.1016/j.tiv.2012.12.023, indexed in Pubmed: 23280101.
44. Ariosa AR, Lahiri V, Lei Y, et al. A perspective on the role of autophagy in cancer. Biochim Biophys Acta Mol Basis Dis. 2021; 1867(12): 166262, doi: 10.1016/j.bbadis.2021.166262, indexed in Pubmed: 34481059.
45. Zhang Bo, Liu L. Autophagy is a double-edged sword in the therapy of colorectal cancer. Oncol Lett. 2021; 21(5): 378, doi: 10.3892/ol.2021.12639, indexed in Pubmed: 33777202.
46. Chen Y, Chen HN, Wang K, et al. Ketoconazole exacerbates mitophagy to induce apoptosis by downregulating cyclooxygenase-2 in hepatocellular carcinoma. J Hepatol. 2019; 70(1): 66–77, doi: 10.1016/j.jhep.2018.09.022, indexed in Pubmed: 30287340.
47. Wang X, Liu Q, Wang Z, et al. Role of autophagy in sonodynamic therapy-induced cytotoxicity in S180 cells. Ultrasound Med Biol. 2010; 36(11): 1933–1946, doi: 10.1016/j.ultrasmedbio.2010.06.022, indexed in Pubmed: 20888686.

Submitted: 23 April, 2023
Accepted after reviews: 24 September, 2023
Available as AoP: 3 October, 2023